Pergamon

Bioorganic & Medicinal Chemistry 7 (1999) 2727–2735

BIOORGANIC & MEDICINAL CHEMISTRY

Pseudo-Cyclic Oligonucleotides: In Vitro and In Vivo Properties

Zhiwei Jiang,[a] Ekambar R. Kandimalla,[a] Qiuyan Zhao,[a] Ling X. Shen,[a,1] Antonella DeLuca,[b] Nicola Normano,[b] Mary Ruskowski[c] and Sudhir Agrawal[a,*]

[a]*Hybridon, Inc., 155 Fortune Boulevard, Milford, MA 01757, USA*
[b]*Oncologia Sperimentale D, ITN-Fondazione, Pascale, Naples, Italy*
[c]*Department of Nuclear Medicine, University of Massachusetts Medical Center, 55 Lake Avenue North, Worcester, MA 01655, USA*

Received 28 April 1999; accepted 24 June 1999

Abstract—We have designed and studied antisense oligodeoxynucleotides (oligonucleotides; oligos) which we call 'pseudo-cyclic oligonucleotides' (PCOs). PCOs contain two oligonucleotide segments attached through their 3′-3′- or 5′-5′-ends. One of the segments of the PCO is an antisense oligo complementary to a target mRNA, and the other is a short protective oligo that is 5–8 nucleotides long and complementary to the 3′- or 5′-end of the antisense oligo. As a result of complementarity between the antisense and protective oligo segments, PCOs form intramolecular pseudo-cyclic structures in the absence of the target RNA. The antisense oligo segment of PCOs used for the studies described here is complementary to an 18-nucleotide-long site on the mRNA of the protein kinase A regulatory subunit RIα (PKA-RIα). Thermal melting studies of PCOs in the absence and presence of the complementary RNA suggest that the pseudo-cyclic structures formed in the absence of the target RNA dissociate, bind to the target RNA, and form heteroduplexes. The results of RNase H cleavage assays suggest that PCOs bind to complementary RNA and activate RNase H in a manner similar to that of an 18-mer conventional antisense PS-oligo. In snake venom (a 3′-exonuclease) or spleen (a 5′-exonuclease) phosphodiesterase digestion studies, PCOs are more stable than conventional antisense oligos because of the presence of 3′-3′- or 5′-5′-linkages and the formation of intramolecular pseudo-cyclic structures. PCOs with a phosphorothioate antisense oligo segment inhibited cell growth of MDA-MB-468 and GEO cancer cell lines similar to that of the conventional antisense PS-oligo, suggesting efficient cellular uptake and target binding. The nuclease stability studies in mice suggest that PCOs have higher in vivo stability than antisense PS-oligos. The studies in mice showed similar pharmacokinetic and tissue distribution profiles for PCOs to those of antisense PS-oligos in general, but rapid elimination from selected tissues.

Introduction

Progress in the discovery and development of antisense oligonucleotides as therapeutic agents is continuing at a rapid pace.[1–6] For the effective use of an oligonucleotide, it must interact with the target mRNA by Watson–Crick base pairing, activate RNase H for mRNA cleavage, be stable towards nucleases, and be taken up by cells efficiently.[2–5] Oligodeoxynucleotide phosphorothioates (PS-oligos) possess all these properties and have been studied extensively for their in vitro and in vivo biological activity,[3–10] safety,[2,11–13] and pharmacokinetic profiles.[13–18] The potential application of PS-oligos as therapeutic agents is currently being evaluated in a number of human clinical trials.[3–6] In order to further improve the potential of PS-oligos as antisense agents, various mixed-backbone oligonucleotides (MBOs) have been introduced and evaluated.[19–23] In MBOs, desirable properties of PS-oligos are maintained while undesirable properties are minimized by a combination of modifications in oligonucleotides. MBOs containing 2′-*O*-alkylribonucleotides have been studied extensively and have yielded promising results in terms of biological activity and general toxicity.[21,24,25] In addition, MBOs have shown significant increase in in vivo stability compared to PS-oligos, which has allowed administration by oral route[26] and may allow less frequent administration by other routes. Based on their advantages over PS-oligos, MBOs have become the first choice of second-generation antisense oligonucleotides and are currently being studied for their potential in human clinical trials.

In continuation of our efforts to improve the properties of PS-oligos as therapeutic agents, we have considered

Key words: Antisense; in vivo stability; oligonucleotides; pharmacokinetics.
* Corresponding author. Tel.: +508-482-7530; fax: +508-482-7692; e-mail: sagrawal@hybridon.com
[1] Present address: Variagenics, Inc., 60, Hampshire Street, Cambridge, MA 02139, USA.

0968-0896/99/$ - see front matter
PII: S0968-0896(99)00217-5

structural changes in PS-oligos. In our earlier studies we reported self-stabilized oligonucleotides, a PS-oligo containing a hairpin loop region at the 3′-end which provided increased in vivo nuclease stability and improved biological activity, and more importantly improvement in toxicity compared to a PS-oligo without a secondary structure at the 3′-end.[11,27–29] Follow up studies by others have also yielded encouraging results.[30]

To further improve the properties of PS-oligos, we report here the design of antisense oligonucleotides referred to as 'pseudo-cyclic oligonucleotides' (PCOs). In PCOs, two oligonucleotides are linked to each other by a 3′-3′-linkage, one oligonucleotide of which is antisense to the target mRNA and the other is a protective oligonucleotide complementary to five to eight nucleotides at the 5′-end of the antisense oligonucleotide (Fig. 1).

Under physiological conditions in the absence of target mRNA, PCOs adopt an intramolecular cyclic or pseudo-cyclic structure as a result of complementarity between antisense and protective oligos, as shown in Figure 1. The 3′-3′-linkage between protective and antisense oligos provides increased nuclease stability from the 3′-end. The pseudo-cyclic structure formation at the 5′-end imparts additional nuclease stability against 5′-nucleases. The PCOs may stay in linear form or hybridized form (Fig. 1) depending on the temperature, salt concentration, and length of the protective oligonucleotide. If the PCO is in the intramolecular pseudo-cyclic form, it may exhibit fewer of the polyanionic-related side effects (e.g. complement activation and prolongation of partial thromboplastin time) known to occur with PS-oligos, because there are fewer exposed phosphorothioate linkages. The new design is aimed to improve pharmacokinetic and tissue distribution and increase elimination of antisense oligos from tissues, in addition to reducing polyanion related side effects, while retaining similar biophysical, biochemical and biological properties as that of PS-oligos.

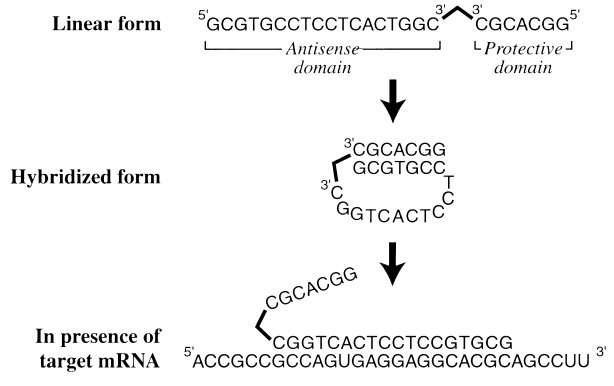

Figure 1. Graphical representation of oligonucleotides showing two regions of pseudo-cyclic oligonucleotide (PCO) — an antisense oligo and a protective oligo. In pseudo-cyclic form, the antisense and protective oligos of a PCO hybridize to each other. In the presence of a complementary RNA, the PCO adopts a linear form because of the higher stability of the heteroduplex between antisense oligo and the target RNA.

To study the potential of PCOs, we have used a PS-oligo (18-mer) complementary to the regulatory subunit of PKA-RIα.[31] An antisense oligonucleotide complementary to this region of PKA-RIα mRNA has been studied in detail in vitro and in vivo models[31–33] and is currently being evaluated in human clinical trials.[34]

Results and Discussion

The 18-mer PS-oligo (**1**) (Table 1) that is complementary to the mRNA of regulatory subunit of protein kinase A (RIα) used in this study has been shown to be effective in inhibiting the growth of various cancer cells in vitro and the growth of tumors in mouse xenograft models by a sequence-specific antisense mechanism.[31–36] We have synthesized two sets of oligonucleotides that contain (1) phosphodiester backbones in both antisense and protective oligo segments (5′-5′- and 3′-3′-orientations), and (2) phosphorothioate backbone in the antisense oligo segment and phosphodiester backbone in the protective oligo segment (3′-3′ orientation). The first set with phosphodiester backbones in both the oligo segments was used for evaluating preliminary in vitro properties, and the second set was used to evaluate in vitro as well as in vivo properties.

PCOs containing phosphodiester antisense segment

First, we synthesized oligo **2** (Table 1), which has an 18-mer phosphodiester oligonucleotide (PO-oligo) as the antisense oligonucleotide and a 6-mer as the protective PO-oligo linked by their 5′-5′-ends. As a control, we synthesized oligo **3** (Table 1), in which the antisense oligonucleotide is the same as in oligo **2**, but which contains two mismatches in the protective PO-oligo.

Thermal melting studies. The T_m value of oligo **2** alone was 51.9°C, whereas oligo **3** alone showed a broad transition without a defined T_m value, indicating that antisense oligonucleotide hybridizes to the complementary 6-mer protective oligonucleotide and forms an intramolecular pseudo-cyclic structure, as shown in Figure 1. Alternately, oligo **2** can form linear tandem and/or cyclic intermolecular complexes under experimental conditions. However, the non-denaturing polyacrylamide gel and concentration-dependent thermal melting experiments suggest formation of only intramolecular cyclic structures and not intermolecular cyclic or linear tandem structures (data not shown). Oligo **3**, which had two mismatches in the protective oligonucleotide, fails to hybridize with the antisense oligonucleotide and remains in the linear form.

In the presence of the complementary RNA (5′-CUGUGAGUGAGAACAGGUGUCACCU-3′), oligos **2** and **3** had T_m values of 76.7 and 76.8°C, respectively, suggesting that the antisense oligonucleotides of oligos **2** and **3** hybridized to the target RNA and formed stable heteroduplexes. The T_m values were recorded by mixing the hybridized form of oligo **2** and the complementary RNA at room temperature (21°C) rather than heating to 85°C, and then cooling the mixture to

Table 1. Oligonucleotide sequences, secondary structures and T_ms in the absence and presence of the target RNA

Oligo no.	Sequence[a]	Secondary structure[b]	T_m (°C) in the absence and presence of RNA[c]	
			Absence	Presence
1	5'-GCGTGCCTCCTCACTGGC-3'		—	67.7
2	3'-CGGTCACTCCTCCGTGCG-5'-5'-GCCAGT-3'	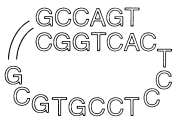	51.9	74.8
3	3'-CGGTCACTCCTCCGTGCG-5'-5'-GCGAAT-3'	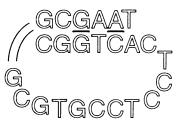	bt	76.3
4	5'-GCGTGCCTCCTCACTGGC-3'-3'-CGCACG-5'		56.5	76.7
5	5'-GCGTGCCTCCTCACGGC-3'-3'-GGAACC-5'		bt	76.8
6	5'-GCGTGCCTCCTCACTGGC-3'-3'-CGCAC-5'	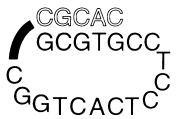	bt	66.9
7	5'-GCGTGCCTCCTCACTGGC-3'-3'-CGCACG-5'	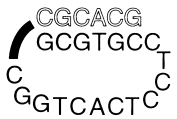	48.0	68.1
8	5'-GCGTGCCTCCTCACTGGC-3'-3'-CGCACGG-5'	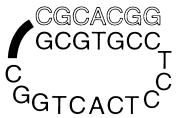	50.2	67.1
9	5'-GCGTGCCTCCTCACTGGC-3'-3'-CGCACGGA-5'	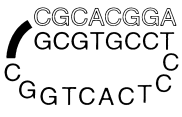	55.3	67.4
10	5'-GCGTGCCTCCTCACTGGC-3'-3'-GGAAC-5'		bt	68.3
11	5'-GCGTGCCTCCTCACTGGC-3'-3'-GGAACAG-5'	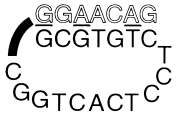	bt	68.2

[a] Open and plain letters represent phosphodiester (PO) and phosphorothioate (PS) linkages, respectively; underlined bases represent mismatches.

[b] // and) represent 5′-5′- and 3′-3′-linkages, respectively.

[c] See Experimental for buffer conditions; bt represents broad transition without a defined melting temperature.

destabilize the intramolecular pseudo-cyclic structure of oligo **2** to favor duplex formation with the RNA. These results suggest that the intramolecular pseudo-cyclic structure of oligo **2** destabilizes by itself in the presence of the complementary RNA and forms a stable heteroduplex. The thermal stability of the duplex of oligo **2** and the RNA was higher than the thermal stability of the intramolecular pseudo-cyclic structure of oligo **2** (Table 1), which would also favor destabilization of the pseudo-cyclic structure of oligo **2**.

In vitro nuclease stability. To determine if the pseudo-cyclic form of oligo **2** confers upon it greater nuclease stability than found with oligo **3**, both oligos **2** and **3** were incubated with snake venom phosphodiesterase (SVPD). Aliquots of the incubation mixtures were removed at 0, 5 and 30 min, and analyzed by CGE. Figure 2 shows that oligo **2** was relatively more stable than oligo **3**: intact oligo **2** was still detectable after 30 min, whereas oligo **3** was completely degraded even at the 5-min time point under the same experimental conditions. These results suggest that in spite of the presence of two 3′-ends in these oligos, only oligo **2** is more stable against the 3′-exonuclease SVPD, because of the presence of the intramolecular pseudo-cyclic structure.

In the next step we synthesized and studied oligos **4** and **5** in which antisense and protective PO-oligos were linked by 3′-3′-linkages. Oligos **4** and **5** had T_m values similar to those of oligos **2** and **3**, respectively (Table 1). In nuclease stability experiments against spleen phosphodiesterase (a 5′-exonuclease), oligo **4**, which exists in a pseudo-cyclic form, was more stable (as in the case of oligo **2**); oligo **5**, which cannot form intramolecular pseudo-cyclic structures, was digested completely (as in the case with oligo **3**; data not shown). These results suggest that pseudo-cyclic structure formation provides antisense oligonucleotides with increased stability against exonucleases than terminally protected oligonucleotides in vitro[37] and in vivo.[38,39]

PCOs containing phosphorothioate antisense segment

Encouraged by these results, we synthesized oligos **6–9**, which consisted of 18-mer PS-oligo as the antisense oligonucleotide and PO-oligo as the protective oligonucleotide linked through their 3′-ends (3′-3′-linkage) to evaluate further for their in vitro and also in vivo properties. Although several modifications can be used in the protective oligo region, in the present study we used phosphodiester modification in order not to increase the phosphorothioate content of the oligo. The length of the protective oligo varied from 5- to 8-mer (oligos **6–9**, respectively) (Table 1). As controls, we synthesized oligos **10** and **11** containing two and three mismatches, respectively, in the protective oligonucleotide. These controls corresponded to oligos **6** and **9** in length. Oligo **1**, an 18-mer PS-oligo without a protective oligonucleotide appendage, was synthesized for comparison.

Thermal melting studies. Thermal melting studies showed that oligo **6** alone had a broad transition, whereas oligos **7–9** alone had T_m values of 48, 50.2 and 55.3°C, respectively. These results suggest that oligo **6**, in which the protective oligonucleotide was only five nucleotides long, did not form a stable pseudo-cyclic structure with the 5′-region of the antisense oligonucleotide (PS-oligo). The stability of the pseudo-cyclic structures of oligos **7–9**, in which the length of protective oligonucleotide increased from six bases to eight bases long, respectively, increased progressively. Oligos **10** and **11**, which contained mismatches in the protective oligo segment, showed broad melting transitions without definitive T_m values. In the presence of the complementary RNA, oligos **6–11** showed similar T_m values (Table 1), suggesting that all oligos adopted the linear form in the presence of RNA and formed heteroduplexes.

RNase H assay. Opening of cyclic structures of PCOs in the presence of target RNA was further confirmed by an experiment in which oligos **6–11** were incubated with

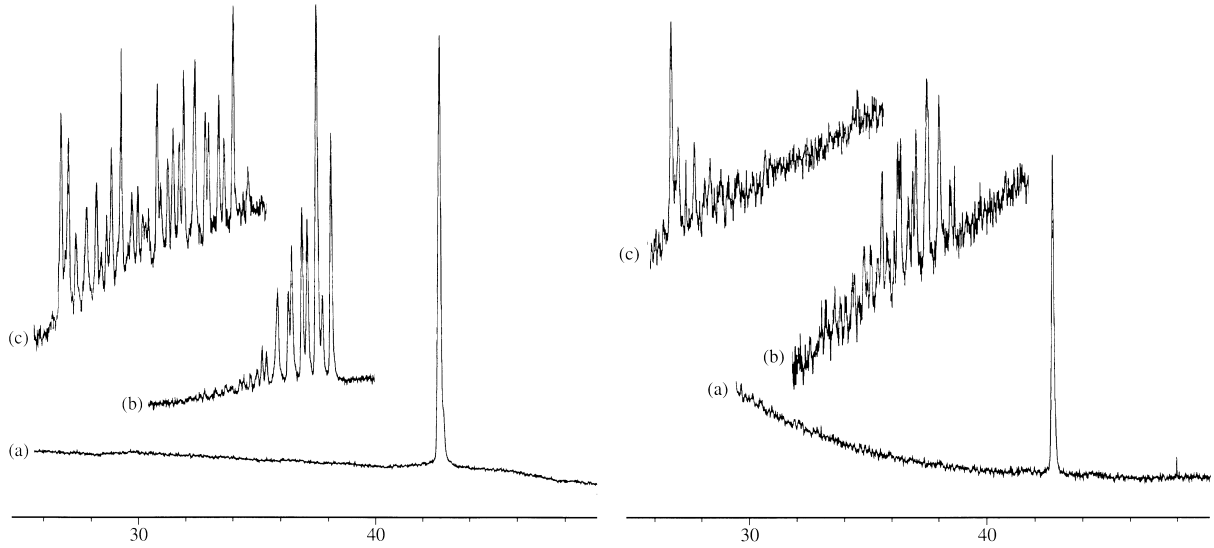

Figure 2. Capillary gel electrophoresis profiles of oligos **2** (left panel) and **3** (right panel) in the presence of snake venom phosphodiesterase at time points (a) 0 min, (b) 5 min, and (c) 30 min in both the panels. In all the panels the late eluted peak corresponds to intact oligo.

the complementary RNA that was labeled at the 5′-end with ^{32}P and *Escherichia coli* RNase H. RNase H binds to the DNA–RNA heteroduplex and cleaves RNA at the 3′-end of the RNA of the heteroduplex.[23,40] The cleavage pattern of RNA in the presence of oligos **6**–**11** was similar to that of oligo **1** (Fig. 3), suggesting that these oligos adopted a linear form in the presence of the complementary RNA and that all oligonucleotides formed heteroduplexes with the target RNA; these heteroduplexes were substrates for RNase H, which is one of the important properties required for antisense activity.

Inhibition of cell growth. Having established that these oligonucleotides formed intramolecular pseudo-cyclic structures under physiological conditions and adopted a linear form and bound to the target in the presence of the complementary RNA, we performed further experiments to determine if the pseudo-cyclic structures would be taken up by cells, bind to the mRNA, and ultimately exert biological activity similar to that of oligo **1**, which does not have a protective oligo appendage and also does not form any intramolecular structures. Studies were carried out using oligos **1**, **6** and **8** to examine inhibition of cancer cell growth of MDA-MB-468 (breast cancer) and GEO (colon cancer) cell lines using anchorage-dependent and anchorage-independent assays. In these assay systems, use of lipids is not required for delivery of oligonucleotides.[41,42] In addition, we wanted to avoid the use of lipids, because PCOs have variable polyanionic natures, and their encapsulation with lipids may not be consistent. Oligo **1** has been extensively studied against a number of cancer cell lines and has been shown to inhibit cell growth by an antisense mechanism.[31–33,35,36] Results of percentage growth inhibition using these oligonucleotides are summarized in Figure 4. All oligonucleotides showed similar dose-dependent growth inhibitory activity. These results confirm that oligos **6** and **8**, which have the same antisense sequence as that of oligo **1**, had similar cell growth inhibitory activity and that the protective oligonucleotide portion of oligos **6** and **8** did not interfere in their biological activity. Future studies will focus on exploring non-sequence-specific activities, if any, of the protective oligonucleotide portion with appropriate controls.

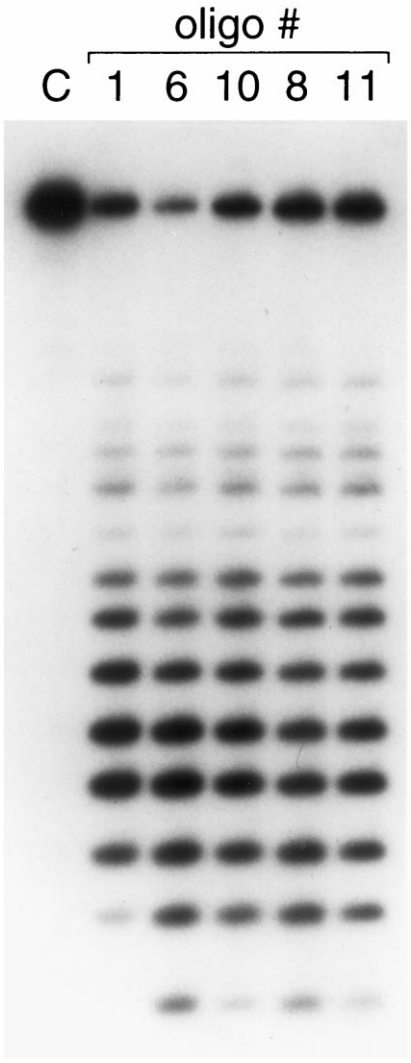

Figure 3. RNase H cleavage profile of 5′-^{32}P-labeled RNA in the presence of oligos **1**, **6**, **8**, **10** and **11** in lanes 2–6, respectively. Lane 1, labeled C, represents control in the absence of antisense oligonucleotide. The slowest moving band on the gel represents intact RNA.

In vivo nuclease stability. Having established that oligos **7**–**9** adopt intramolecular pseudo-cyclic forms under physiological conditions, adopt a linear form in the presence of the complementary RNA, maintain binding affinity to activate RNase H, and have biological activity, we were interested in examining the in vivo nuclease stability of these oligonucleotides compared to oligo **1**. We studied three oligos, **1**, **6** and **8**, for their comparative in vivo stability. We administered these three oligos intravenously to mice at a dose of 50 mg/kg. At 1 and 3 h after administration, blood was collected in heparinized tubes and plasma samples were prepared. Oligonucleotides were extracted from the plasma using the protocols reported earlier[43] and labeled with ^{32}P using polynucleotide kinase. The analysis of the labeled oligonucleotides by polyacrylamide gel electrophoresis showed the presence of intact as well as degradation products of oligos **1**, **6** and **8** in plasma (Fig. 5). Analysis of the results of oligos **6** and **8** showed primarily the presence of bands with slower mobility than intact 18-mer oligo **1**, while oligo **1** showed the presence of degradation products, suggesting that the 3′-3′-linkage between the protective and the antisense oligonucleotides provides increased nuclease stability. It is worth mentioning that degradation of oligos **6** and **8** produces an 18-mer PS-oligonucleotide (oligo **1**) that contains at least one nucleotide attached via a 3′-3′-linkage as the intermediate product, which will also provide increased stability, even after degradation of protective oligo (see Fig. 5).

Pharmacokinetic and tissue disposition. The above results show that oligos **6** and **8** have increased in vivo stability compared to oligo **1** and that the increase in stability of oligos **6** and **8** is the result of formation of intramolecular pseudo-cyclic structures (oligo **8**) under physiological conditions as well as protection of 3′-end

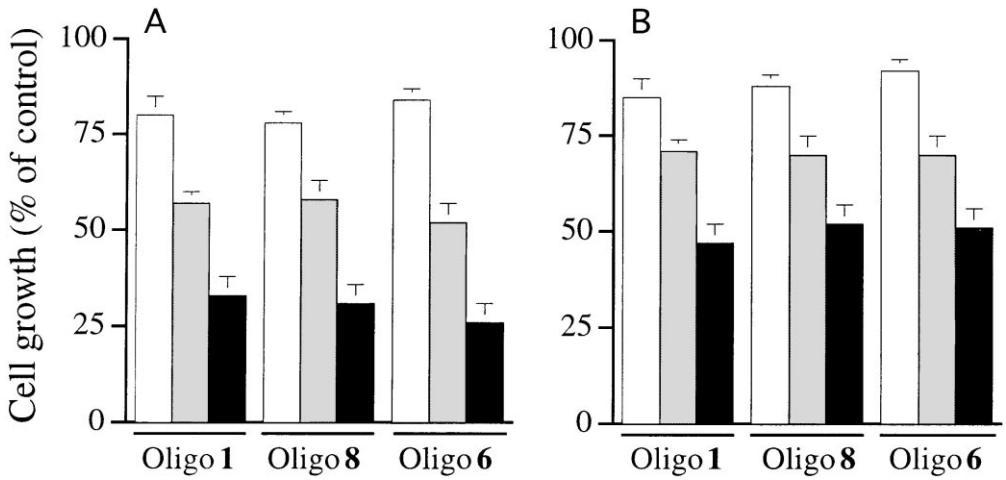

Figure 4. Inhibition of (A) anchorage-independent growth of GEO cancer cells and (B) anchorage-dependent growth of MDA-MB-468 cancer cells by oligos **1**, **6** and **8** at 0.2 μM (no shade), 0.5 μM (light shade) and 1 μM (dark shade).

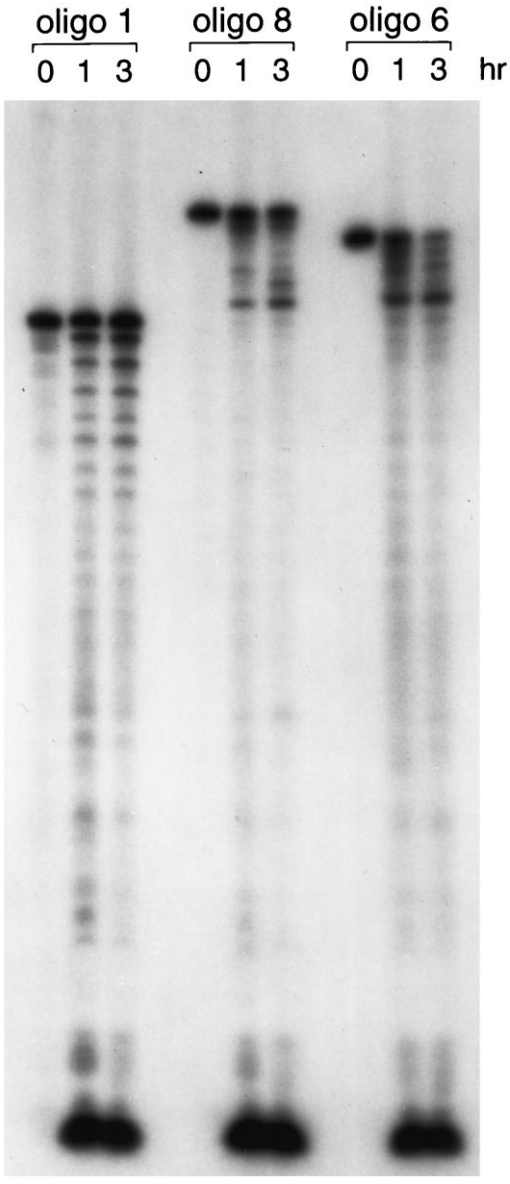

Figure 5. In vivo stability of oligos **1**, **6** and **8** in plasma at 1 h (lane 2) and 3 h (lane 3) after administration to mice.

by 3′-3′-linkage (oligos **6** and **8**). We undertook a preliminary pharmacokinetic tissue disposition study of oligo **8** in mice. We administered 2 mg/kg of oligo **8** (a mixture of ^{35}S-labeled and unlabeled oligo) subcutaneously to mice to understand if there are any significant differences in pharmacokinetic and tissue distribution profiles compared to PS-oligos in general. At 3, 48 and 96 h after administration, mice were sacrificed and liver, kidney, heart, lung and spleen were collected. Tissues were homogenized and radioactivity levels were quantitated. Concentration of oligo **8** based on the radioactivity levels in tissues is presented in Figure 6A and B. It shows that oligo **8** was distributed to major organs and the tissue disposition profile was similar to what has been reported for other PS-oligos.[16–18] However, notable changes were observed in clearance from the tissues compared with PS-oligos.[6,14–16] Figure 6A shows the percentage of the administered dose distributed to liver, kidney and spleen at 3, 48 and 96 h. Figure 6C shows more than 60% of the administered dose was excreted in urine in 7 days. Clearance of oligo from tissues was more rapid than what has been observed with PS-oligos in general.[6,14–16] This observation suggests that oligo **8** remains in the intramolecular pseudo-cyclic form in tissues, interacts less with macromolecules, and is thereby rapidly eliminated from these tissues. However, further studies are needed to establish this proposal and such studies are currently underway.

Conclusions

In conclusion, our studies demonstrate that PCOs containing 3′-3′ (or 5′-5′) linkages adopt intramolecular pseudo-cyclic structures under physiological conditions as indicated by thermal melting, and in vitro and in vivo nuclease stability studies. These PCOs adopt a linear form in the presence of complementary target RNA and bind to the target RNA as indicated by thermal melting and RNase H cleavage studies. Preliminary studies show that PCOs maintain similar antisense activity in cell cultures as that of a control antisense PS-oligo. These results showed that PCOs permitted design of

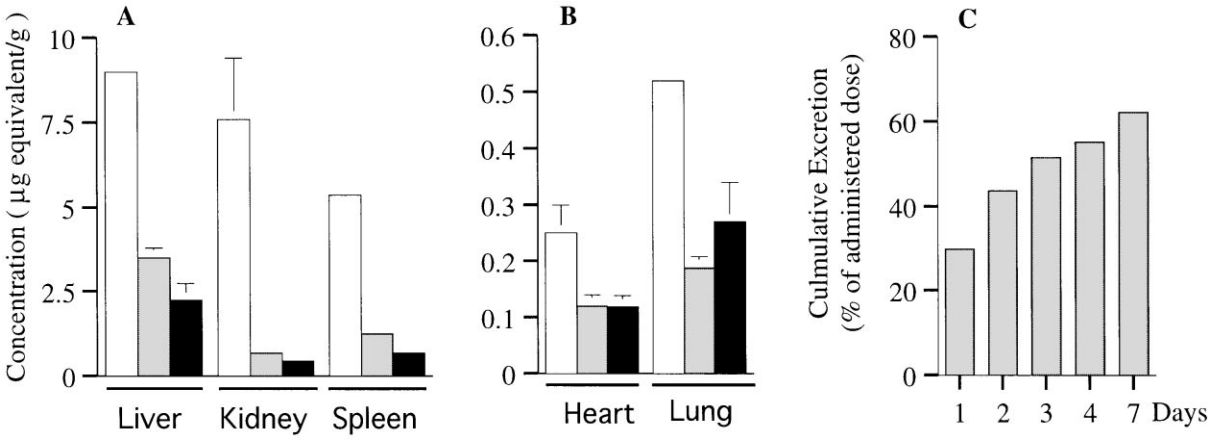

Figure 6. Tissue disposition (A and B) and elimination in urine (C) of oligo **8** following subcutaneous administration to mice. In (A) and (B) no shade, light shade and dark shade bars represent tissue disposition of oligo at 3, 48 and 96 h, respectively, after administration to mice. The data represent mean ± SD from at least two mice.

antisense oligos with similar biophysical and biological properties as those of first generation antisense PS-oligos with favorable pharmacokinetic, tissue distribution and rapid elimination from liver and kidney. The advantage we foresee with PCOs is that their formation of intramolecular pseudo-cyclic structures may allow for less interaction with non-targeted macromolecules (including nucleic acids and proteins) and also reduced polyanionic-related side effects, and will linearize in the presence of the target mRNA only. Further studies are ongoing to fully evaluate the potential of PCOs as effective antisense agents.

Experimental

Synthesis and analysis of oligonucleotides

The synthesis of oligonucleotides was carried out on a 1-µmol scale on a Biosearch 8900 DNA synthesizer using deoxynucleoside-3′-phosphoramidites (PE Biosystems, Framingham, MA) for chain elongation from the 3′- to 5′-end and deoxynucleoside-5′-phosphoramidites (Glen Research, Sterling, VA) for chain elongation from the 5′- to 3′-end. All oligonucleotides, except oligo **1**, were synthesized in two steps. First, oligonucleotides (except oligos **2** and **3**) were synthesized from the 5′- to the 3′-end by using 3′-dimethoxytrityl-deoxynucleoside-CPG (Glen Research, Sterling, VA) and appropriate deoxynucleoside-5′-phosphoramidites using a modified RNA synthesis program in which the detritylation time and detritylation solution volume were doubled compared to the standard RNA synthesis program. The second part of the oligonucleotides (except for oligos **2** and **3**) was synthesized from the 3′- to the 5′-end by using deoxynucleoside-3′-phosphoramidites and a standard DNA synthesis program. Oligos **2** and **3** were synthesized first from the 3′- to the 5′-end, then from the 5′- to the 3′-end using appropriate CPG support bound nucleoside, nucleosidephosphoramidites, and a synthesis program. Oligo **1** was synthesized using deoxynucleoside-3′-phosphoramidites and a standard DNA synthesis program. Oxidation following each coupling was carried out using 3H-1,2-benzodithiol-3-one-1,1-dioxide to obtain a phosphorothioate linkage or using iodine reagent to obtain a phosphodiester linkage as desired. Deprotection of all oligonucleotides was completed by incubating with the concentrated ammonium hydroxide solution at 65°C overnight. Oligonucleotides were purified using preparative polyacrylamide gel electrophoresis and desalted using C_{18} Sep-Pak cartridges (Waters). Analysis of the oligonucleotides was carried out using capillary gel electrophoresis (CGE). The purity of the oligonucleotides based on A260/mass ratio was >98%, and based on CGE was 95%, the rest being *n*-1, *n*-2, etc. products. The concentrations of the oligonucleotides were determined by measuring absorbances at 260 nm and using extinction coefficients, which were calculated by the nearest neighbor method.[44]

Synthesis of ^{35}S-labeled oligonucleotide

For ^{35}S-labeling, oligo **8**, which contained four H-phosphonate linkages at the 5′-end of antisense oligonucleotide, was synthesized. For labeled product, synthesis of oligo **8** was carried out in three steps: the first and second steps were carried out as described above. In the third step, the last four couplings were carried out using nucleoside-H-phosphonates and H-phosphonate chemistry. Oxidation of the last four H-phosphonate linkages was carried out with ^{35}S-elemental sulfur (0.5–2.5 Ci/mg, Amersham) as reported earlier.[16] ^{35}S-Labeled oligo **8** was purified using preparative 20% polyacrylamide gel electrophoresis and desalted using C_{18} Sep-Pak cartridges. The specific activity of oligo **8** obtained was 0.2 µCi/µg.

Thermal melting experiments

Melting temperatures of oligonucleotides alone and in the presence of complementary RNA were determined in a buffer containing 100 mM NaCl, 2 mM $MgCl_2$, 0.1 mM Na_2EDTA, and 10 mM sodium phosphate, pH 7.4.[22,23] Each oligonucleotide was taken alone or mixed with complementary RNA (5′-CUGUGAGUGAGAACAGGUGUCACCU-3′) at a 1:1 ratio in an

eppendorf tube and dried in a speed vac, and resuspended in 1 mL of buffer. The final concentration of the oligonucleotide and the complementary RNA was 1 μM each. The samples containing oligo alone were heated at 85°C for 2 min, and cooled immediately on ice for 5 min to allow formation of intramolecular duplexes. The samples containing oligo with the complementary RNA were incubated at room temperature (21°C) for 1 h. Then the UV absorbance curves as a function of temperature were recorded on a Lambda 20 UV–vis spectrometer (Perkin–Elmer) at 260 nm using a linear movement multicell holder (6 cells). The temperature was controlled by a PTP-6 Peltier System attached to the spectrometer. The heating rate was 0.5°C/min. The data were collected on a Dell computer interfaced with the instrument and processed with UV-WinLab software which came with the instrument. The melting temperatures (T_ms) were measured from first derivative curves. Each T_m value was an average of at least two measurements and the reproducibility was within ± 1.0°C.

Nuclease-stability of oligonucleotides

One A_{260} unit of oligonucleotide was heated to 90°C for 2 min in a buffer containing 100 mM NaCl, 2 mM $MgCl_2$, 25 mM Tris–HCl, pH 7.5, and then cooled down quickly to 0°C. The annealed samples were incubated with snake venom phosphodiesterase (0.1 μg, Boehringer Mannheim) at 37°C for 5 or 30 min. The digestion was stopped by heating to 90°C for 5 min. The digested oligos were desalted using C_{18} Sep-Pak cartridges before analysis by CGE (Model 2200, Beckman Instruments).

RNase H mediated cleavage experiments

RNA was labeled with ^{32}P at the 5′-end using T4 polynucleotide kinase (Pharmacia) and [γ-^{32}P]ATP (Amersham), as reported earlier.[23] Oligos **1**, **6**, **8**, **10** and **11** were dissolved in 10 μL buffer (30 mM Hepes/KOH, pH 8.0, 75 mM KCl, 6 mM $MgCl_2$, 1.5 mM DTT, 75 μg/mL BSA), heated at 85°C for 1 min and then cooled on ice for 5 min. About 50,000 cpm of ^{32}P-end labeled RNA (5′-CUGUGAGUGAGAACAGGU-GUCACCU-3′) in 4 μL of water was added to the annealed oligonucleotide in buffer solution (10 μL), and incubated at 37°C for 10 min. *E. coli* RNase H (0.65 μL of 1:10 diluted, Pharmacia) was added to the mixture and incubated at 37°C for 10 min. The reaction was stopped by the addition of 1 μL of 0.5 M EDTA and 20 μL of formamide and analyzed using 20% denaturing polyacrylamide gel electrophoresis and autoradiography.

In vivo stability of oligos

Oligos **1**, **6** and **8** were administered intravenously to CD-1 mice (20–25 g) at a dose of 50 mg/kg. Blood was collected from mice at 1 and 3 h after administration in heparinized tubes. The plasma (100 mL) was incubated with proteinase K (60 μg, Sigma) in extraction buffer (0.5% SDS, 10 mM NaCl, 20 mM Tris–HCl, pH 7.6, 10 mM EDTA) for 2 h at 60°C. The samples were extracted twice with phenol:chloroform (1:1, v/v) and precipitated with ethanol after addition of glycogen (1 μg). The samples were 5′-end labeled with [γ-^{32}P]ATP (Amersham) using T4 polynucleotide kinase (10 units, New England Biolabs) and then analyzed using 20% denaturing polyacrylamide gel electrophoresis and autoradiography.

Pharmacokinetics and tissue disposition

Oligo **8** was administered subcutaneously at a dose of 2 mg/kg (a mixture of unlabeled and ^{35}S-labeled oligo **8**) in 100 μL saline to CD-1 male mice (20–24 g, Charles River, Wilmington, MA). At 3, 48 and 96 h after administration, two mice at each time point were euthanized by exposure to metofane (Malinkrodt Veterinary, Mundelein) followed by cervical dislocation. Blood was collected in EDTA containing tubes (Becton Dickinson, Franklin Lakes, NJ). Liver, kidney, spleen, heart and lungs were removed and blotted on a piece of gauze, weighed and stored at −20°C. For counting of ^{35}S, 50 μL of plasma was added to 1 mL TS-2 (Research Product International, Mt Prospect, IL), swirled and mixed with 250 μL 10% glacial acetic acid. The sample was swirled again until uniform, then 18 mL of 3a70B scintillation cocktail (Research Product International) was added. Samples were prepared in triplicate and incubated overnight at room temperature before counting. Pieces of tissues in triplicate, weighing between 10 and 50 mg, were placed in scintillation vials to which was added 1 mL of tissue solubilized TS-2. The vials were incubated for 2–4 h at 50°C, mixed with 250 μL of 10% glacial acetic acid; after mixing, 18 mL of 3a70B scintillation cocktail was added. The vial was again swirled and left overnight to diminish chemiluminescence. The radioactivity level was counted using a Beckman liquid scintillation counter.

Inhibition of cell growth

Cell culture: MDA-MB-468 human breast cancer cells were procured from the American Type Culture Collection (Rockville, MD). The cells were routinely maintained in a 1:1 (v/v) mixture of Dulbecco's modified eagle's medium (DMEM) and Ham's F12 medium supplemented with 10% heat-inactivated fetal calf serum, 20 mM Hepes (pH 7.4), penicillin (100 U/mL) and streptomycin (100 μg/mL) (Flow, Irvine, UK). GEO cells were kindly provided by Dr. M. Brattain (Baylor College of Medicine, Houston, TX). GEO cells were maintained in McCoy's medium supplemented with 10% heat-inactivated fetal bovine serum, 20 mM Hepes (pH 7.4), penicillin (100 U/mL) and streptomycin (100 μg/mL) in a humidified atmosphere of 95% air and 5% CO_2 at 37°C.

Anchorage-dependent growth assay. The assay was carried out as reported earlier.[39] Typically, MDA-MB-468 cells (10^4 cells/well) were seeded into 48-multiwell cluster dishes (Becton Dickinson, Milan, Italy) and treated every 24 h with the indicated concentrations of oligos. After 5 days of growth, the cells were trypsinized and counted with a hemocytometer.

Clonogenic assay. GEO cells (5×10^3 cells/well) were seeded in 0.3% Difco bactoagar (Difco, Detroit, MI) supplemented with complete culture, as reported earlier.[38] This suspension was layered over 0.5 m of 0.8% agar-medium base layer in 24-multiwell cluster dishes (Becton Dickinson, Milan, Italy). After 12 days, the colonies were stained with nitroblue tetrazolium, and colonies larger than 50 μm were counted with an Artek 880 colony counter (Artek Systems, Farmingdale, NY).

Acknowledgements

The research work carried out in the laboratory of N.N. was supported by a grant from the Associazione Italiana per la Ricerca sul Cancro (AIRC).

References

1. Zamecnik, P. C.; Stephenson, M. L. *Proc. Natl. Acad. Sci. USA* **1978**, *75*, 280.
2. Agrawal, S.; Zhao, Q. *Cur. Opin. Chem. Biol.* **1998**, *2*, 519.
3. Kronenwett, R.; Haas, R. *Ann. Hematol.* **1998**, *77*, 1.
4. Gewirtz, A. M.; Sokol, D. L.; Ratajczak, M. Z. *Blood* **1998**, *92*, 712.
5. Bennett, C. F. *Biochem. Pharmacol.* **1998**, *55*, 9.
6. Ciba Foundation Symposium. *Oligonucleotides as Therapeutic Agents*; John Wiley; New York, 1997.
7. Chen, L.; Agrawal, S.; Zhou, W.; Zhang, R.; Chen, J. *Proc. Natl. Acad. Sci. USA* **1998**, *95*, 195.
8. Masood, R.; Cai, I.; Zheng, T.; Smith, D. L.; Naidu, Y.; Gill, P. S. *Proc. Natl. Acad. Sci. USA* **1997**, *94*, 979.
9. Kita, K.; Saito, S.; Morioka, C. Y.; Watanabe, A. *Int. J. Cancer* **1999**, *80*, 553.
10. Osen-Sand, A.; Catsicas, M.; Staple, J. K.; Jones, K. A.; Ayala, G.; Knowles, J.; Grenningloh, G.; Catsicas, S. *Nature* **1993**, *364*, 445.
11. Agrawal, S.; Zhao, Q.; Jiang, Z.; Oliver, C.; Giles, H.; Heath, J.; Serota, D. *Antisense Nucleic Acids Drug Dev.* **1997**, *7*, 575.
12. Henry, S. P.; Leeds, J.; Giclass, P. S. C.; Gillett, N. A.; Pribble, J. P.; Kornbrust, D. J.; Levin, A. A. *Toxicology* **1997**, *120*, 145.
13. Srinivasan, S. K.; Iversen, P. *J. Clin. Lab. Anal.* **1995**, *9*, 129.
14. Grindel, J. M.; Musick, T. J.; Jiang, Z.; Roskey, A.; Agrawal, S. *Antisense Nucleic Acids Drug Dev.* **1998**, *8*, 43.
15. Phillips, J. A.; Craig, S. J.; Bayley, D.; Christian, R. A.; Geary, R.; Nicklin, P. L. *Biochem. Pharmacol.* **1997**, *54*, 657.
16. Agrawal, S.; Temsamani, J.; Tang, J.-Y. *Proc. Natl. Acad. Sci. USA* **1991**, *88*, 7595.
17. Zhang, R.; Diasio, R. B.; Lu, Z.; Jiang, Z.; Galbraith, W.; Agrawal, S. *Biochem. Pharmacol.* **1995**, *49*, 929.
18. Sands, H.; Gorey-Feret, L. J.; Cocuzza, A. J.; Hobbs, F. W.; Chidester, D.; Trainor, G. L. *Mol. Pharmacol.* **1994**, *45*, 932.
19. Inoue, H.; Hayase, Y.; Iwai, S.; Ohtsuka, E. *FEBS Lett.* **1987**, *215*, 327.
20. Metelev, V.; Lisziewich, J.; Agrawal, S. *Bioorg. Med. Chem. Lett.* **1994**, *4*, 2929.
21. Agrawal, S.; Jiang, Z.; Zhao, Q.; Shaw, D.; Cai, Q.; Roskey, A.; Channavajjala, L.; Saxinger, C.; Zhang, R. *Proc. Natl. Acad. Sci. USA* **1997**, *94*, 2620.
22. Kandimalla, E. R.; Manning, A.; Zhao, Q.; Shaw, D. R.; Byrn, R. A.; Sasisekharan, V.; Agrawal, S. *Nucleic Acids Res.* **1997**, *25*, 370.
23. Shen, L. X.; Kandimalla, E. R.; Agrawal, S. *Bioorg. Med. Chem.* **1998**, *6*, 1695.
24. Agrawal, S.; Zhao, Q. *Antisense Nucleic Acids Drug Dev.* **1998**, *8*, 135.
25. Altman, K.-H.; Dean, N. M.; Fabbro, D.; Freier, S. M.; Geiger, T.; Haner, R.; Husken, D.; Martin, P.; Monia, B. P.; Muller, M.; Natt, F.; Nicklin, P.; Phillips, J.; Pieles, V.; Sasmor, H.; Moser, H. E. *Chimia* **1996**, *50*, 168.
26. Agrawal, S.; Zhang, X.; Zhao, H.; Lu, Z.; Yan, J.; Cai, H.; Diasio, R. B.; Habus, I.; Jiang, Z.; Iyer, R. P.; Yu, D.; Zhang, R. *Biochem. Pharmacol.* **1995**, *50*, 571.
27. Tang, J.-Y.; Temsamani, J.; Agrawal, S. *Nucleic Acids Res.* **1993**, *21*, 2729.
28. Agrawal, S.; Temsamani, J.; Tang, J.-Y. In *Delivery Strategies for Antisense Oligonucleotide Therapeutics;* Akhtar, S., Ed.; CRC Press, Boca Raton, FL, 1995, pp 105–121.
29. Zhang, R.; Lu, Z.; Zhang, X.; Diasio, R.; Liu, T.; Jiang, Z.; Agrawal, S. *Clin. Chem.* **1995**, *41*, 836.
30. Abe, T.; Takai, K.; Nakada, S.; Yokota, T.; Takaku, H. *FEBS Lett.* **1998**, *425*, 91.
31. Yokuzaki, H.; Budillon, A.; Tortora, G.; Meissner, S.; Beaucage, S. L.; Miki, K.; Cho-Chung, Y. S. *Cancer Res.* **1993**, *53*, 868.
32. Nesterova, M.; Cho-Chung, Y. S. *Nature Med.* **1995**, *1*, 528.
33. Srivastava, R. K.; Srivastava, A. R.; Park, Y. G.; Agrawal, S.; Cho-Chung, Y.-S. *Breast Cancer Res. Treat.* **1998**, *49*, 97.
34. Chen, H. Antisense 98, Nature Biotechnology Abstract Book, 1998.
35. Tortora, G.; Caputo, R.; Damiano, V.; Bianco, R.; Pepe, S.; Bianco, A. R.; Jiang, Z.; Agrawal, S.; Ciardiello, F. *Proc. Natl. Acad. Sci. USA* **1997**, *94*, 12586.
36. Ciardiello, F.; Caputo, R.; Bianco, R.; Damiano, V.; Pomatico, G.; Pepe, S.; Bianco, A. R.; Agrawal, S.; Mendelsohn, J.; Tortora, G. *J. Natl. Cancer Inst.* **1998**, *90*, 1087.
37. Seliger, H.; Froehlich, A.; Montenarh, M.; Ortigao, J. F. R.; Roesch, H. *Nucleosides and Nucleotides* **1991**, *10*, 469.
38. Temsamani, J.; Tang, J.-Y.; Agrawal, S. *Annl. N.Y. Acad. Sci.* **1992**, *660*, 318.
39. Chaix, C.; Iyer, R. P.; Agrawal, S. *Bioorg. Med. Chem. Lett.* **1996**, *6*, 827.
40. Crouch, R. J.; Dirksen, M.-L. In *Nucleases*, Linn, S. M.; Roberts, R. J., Eds.; Cold Spring Harbor Laboratory, Cold Spring Harbor, NY, 1982, pp 211–241.
41. DeLuca, A.; Selvam, M. P.; Sandomenico, C.; Pepe, S.; Bianco, A. R.; Ciardiello, F.; Salomon, D. S.; Normanno, N. *Int. J. Cancer* **1997**, *73*, 277.
42. DeLuca, A.; Casamassimi, A.; Selvam, M. P.; Losito, S.; Ciardiello, F.; Agrawal, S.; Salomon, D. S.; Normanno, N. *Int. J. Cancer* **1999**, *80*, 589.
43. Temsamani, J.; Roskey, A.; Chaix, C.; Agrawal, S. *Antisense Nucleic Acids Drug Dev.* **1997**, *7*, 159.
44. Puglisi, J. D.; Tinoco, I., Jr. *Methods Enzymol.* **1989**, *180*, 304.